Stability and Diversity of T Cell Receptor Repertoire Usage during Lymphocytic Choriomeningitis Virus Infection of Mice

By Meei Yun Lin and Raymond M. Welsh

From the Department of Pathology and Program in Immunology and Virology, University of Massachusetts Medical School, Worcester, Massachusetts 01655

Summary

Numerous studies have examined T cell receptor (TCR) usage of selected virus-specific T cell clones, yet little information is available regarding the stability and diversity of TCR repertoire usage during viral infections. Here, we analyzed the Vβ8.1 TCR repertoire directly ex vivo by complementarity-determining region 3 (CDR3) length spectratyping throughout the acute lymphocytic choriomeningitis virus (LCMV) infection, into memory, and under conditions of T cell clonal exhaustion. The Vβ8 population represented 30–35% of the LCMV-induced $CD8^+$ T cells and included T cells recognizing several LCMV-encoded peptides, allowing for a comprehensive study of a multiclonal T cell response against a complex antigen. Genetically identical mice generated remarkably different T cell responses, as reflected by different spectratypes and different TCR sequences in same sized spectratype bands; however, a conserved CDR3 motif was found within some same sized bands. This indicated that meaningful studies on the evolution of the T cell repertoire required longitudinal studies within individual mice. Such longitudinal studies with peripheral blood lymphocyte samples showed that (*a*) the virus-induced T cell repertoire changes little during the apoptosis period after clearance of the viral antigens; (*b*) the LCMV infection dramatically skews the host T cell repertoire in the memory state; and (*c*) continuous selection of the T cell repertoire occurs under conditions of persistent infections.

Key words: lymphocytic choriomeningitis virus • memory • T cell receptor • spectratype • mice

Viral infections often induce potent immune responses associated with hyperplasia of T cells, which clear the virus, undergo apoptosis, and return to homeostasis, leaving the host with memory T cells that rapidly respond to the pathogen on subsequent challenge (1). Although many studies have examined the specificities and functions of selected virus-specific T cell clones (2–5), little is known about the diversity of the T cell repertoire in genetically identical hosts responding to infection and how this repertoire changes during the transition between an acute infection and a memory response. The relationship between T cell repertoires during primary and secondary viral infections and the evolution of the T cell response under conditions of clonal exhaustion associated with persistent infections are also not well understood. For instance, Are there changes in the T cell repertoire during the apoptotic phase of the T cell response? How similar is the memory repertoire to that of the acute infection? Does T cell clonal exhaustion under conditions of high antigen dose eliminate all or simply a subpopulation of responding T cells?

The strong T cell response during lymphocytic choriomeningitis virus (LCMV)[1], strain Armstrong (LCMV-ARM) infection of C57BL/6 mice is well characterized and provides a useful system to study the evolution of the TCR repertoire under conditions where antigen is cleared and where an acute T cell response converts into a memory response. The clone 13 variant of the Armstrong strain, which differs from its parent strain by only two amino acids, disseminates broadly in vivo and results in persistent infection and clonal exhaustion of CTL in high doses (6, 7). The $CD8^+$ T cell epitopes of LCMV-ARM and LCMV clone 13 are the same (8), thereby enabling one to compare the evolution of the LCMV-induced TCR repertoire usage during the LCMV-ARM and LCMV clone 13 infec-

[1]*Abbreviations used in this paper:* CDR3, complementarity-determining region 3; EXPT, experiment; GP, glycoprotein; LDA, limiting dilution assay; LCMV, lymphocytic choriomeningitis virus; NP, nucleoprotein; PB, peripheral blood; pCTL, precursor cytotoxic T lymphocyte; PEC, peritoneal exudate cell; pTh, precursor T helper cell; PV, Pichinde virus.

J. Exp. Med. © The Rockefeller University Press • 0022-1007/98/12/1993/13 $2.00
Volume 188, Number 11, December 7, 1998 1993–2005
http://www.jem.org

tions. For the rest of this paper, we use LCMV to represent the LCMV-ARM parent strain, and clone 13 to represent the disseminating variant.

The acute LCMV infection causes a logarithmic expansion of LCMV-specific CTL, peaking at ~1/30 precursor CTL (pCTL) per $CD8^+$ cell at days 8–9 after infection (9). These activated T cells become sensitized to activation-induced cell death and die through apoptosis at days 10–14 after infection (10, 11). Although there is a remarkable reduction in the total number of $CD8^+$ cells, the pCTL frequency per $CD8^+$ cell for each of three immunodominant peptides drops only twofold and thereafter remains stable throughout the lifetime of the mouse (9, 12). The LCMV-specific $CD4^+$ T helper cell precursors (pTh) peak at only about 1/600 $CD4^+$ T cells, but reduction of pTh per $CD4^+$ cell and the stability of LCMV-specific pTh are similar to those observed in the CD8 system (1). In contrast, the CTL memory is lost under conditions of high doses of LCMV clone 13 infection, which induces a transient antiviral CTL response followed by a clonal exhaustion of the virus-specific CTL (7).

Kinetic studies on the pCTL frequencies to three immunodominant peptides have suggested that the LCMV-specific T cell repertoire remains unchanged between day 7 of infection and well into long term memory and that a high frequency of LCMV-specific memory T cells is preserved into memory. However, these data are dependent on the ability of T cells to grow out in limiting dilution assays (LDA), where in vitro manipulation in the functional assays might introduce unknown biases. Recent work using tetrameric MHC molecules to quantify LCMV-specific T cells supports our previous study, which concluded that most of the $CD8^+$ T cells included during LCMV infection are virus specific (13, 14). These studies also support our LDA data that show a substantial skewing of the TCR repertoire toward virus-specific cells in the memory state. However, these studies define T cells in terms of their specificity and do not evaluate any changes in TCR usage that may develop during the progression of an infection. Little is known about the relationship of multiple clones of T cells to each other in a complex multiclonal immune response directed against a number of immunodominant and subdominant peptides.

To evaluate the dynamics of such a multiclonal T cell response to a virus infection we have done a molecular analysis of the TCR repertoire directly ex vivo by complementarity-determining region 3 (CDR3) length spectratyping, a technique initially developed by Pannetier et al. (15). This technique consists of two major steps to analyze the CDR3, which is encoded by the joining of V, D, and J segments and defines much of the TCR specificity (16). First, the RT-PCR reaction with specific Vβ and Cβ primers competitively amplifies, from a bulk population of T cells, TCR with specific Vβ sequences but different CDR3 regions. Second, the PCR products are further analyzed with different labeled Jβ primers in a run-off reaction to yield the size peaks for all the VDJ combinations. The spectrum of size differences across the CDR3 region is known as the spectratype. Since the relative intensity of a given size peak is proportional to the amount of the nonamplified RNA molecules, an increase in the height and area of a particular peak signals expansion of T cell clones. Therefore, one can obtain distinct CDR3 profiles to analyze for changes of the TCR repertoire during infection.

To examine the LCMV-induced T cell repertoire usage, we analyzed the $V\beta8.1^+$ T cell repertoire because it was expanded vigorously during acute LCMV infection. It represents a substantial portion of the $CD8^+$ T cell response and includes T cells with a wide variety of specificities directed against several virus-encoded peptides. Our data indicate that genetically identical mice generate significantly different T cell responses to the same antigens, albeit with some preferential Jβ usage and a conserved TCR motif. This indicates that, unlike LDA and tetrameric MHC–peptide analyses, spectratype comparisons of T cell receptors between mice are uninterpretable and that individual mice must be examined longitudinally for a meaningful analysis of the evolution of T cell responses. We present here such a longitudinal study, and our data support the concepts that (*a*) no further selection of LCMV-induced T cell repertoire occurs after the virus is cleared and during the apoptotic phase of the immune response; (*b*) the LCMV infection alters the host T cell repertoire dramatically and leaves it with a high frequency of LCMV-specific T cells in the memory state; and (*c*) evolution of the T cell response occurs under conditions of clonal exhaustion associated with persistent infection.

Materials and Methods

Virus Preparation. The LCMV-Arm strain and the AN3739 strain of Pichinde virus (PV) were propagated in baby hamster kidney cells, as described previously (17). The highly disseminating LCMV-Arm clone 13 variant was obtained from Dr. M.B.A. Oldstone (Scripps Clinic and Research Foundation, La Jolla, CA) (8).

Infection of Mice. 5–6-wk-old C57BL/6 male mice were purchased from The Jackson Laboratory (Bar Harbor, ME). For viral infection, mice were injected intraperitoneally with 4×10^4 PFU of LCMV or 3×10^6 PFU of PV in a 0.1-ml vol per mouse, or intravenously with 2×10^7 PFU of LCMV clone 13 in a 0.4-ml vol per mouse. To reduce nonspecific T cell activation induced by fetal bovine serum, LCMV and PV were diluted at 1:100 and 1:20, respectively, with phosphate-buffered saline before injection. For secondary LCMV infection, the immune mice at 6–7 wk after infection, before neutralizing antibodies were significantly induced (18), were injected intraperitoneally with 10^7 PFU of LCMV in a 0.2–0.3-ml vol per mouse.

Spleen Cell Preparation and Sorting. Spleen leukocytes were prepared as described previously (19). To isolate $CD8^+V\beta8^+$ cells, 10^8 spleen cells were stained with 50 μl of anti-CD8 PE (PharMingen, San Diego, CA) and 50 μl of anti-Vβ8.1/8.2 FITC (PharMingen) for 30 min on ice and washed twice with RPMI 1640 (Sigma Chemical Co., St. Louis, MO) before sorting. In some experiments $CD4^+$ and $CD8^+$ cells were isolated by staining with 50 μl of anti-CD8 PE and 50 μl of anti-CD4 FITC (PharMingen) before sorting. For staining, 10^6 spleen cells were mixed with anti-CD8 PE and anti-Vβ8.1/8.2 FITC, and then fixed with 1% paraformaldehyde (J.T. Baker, Inc., Phillipsburg,

NJ). After staining, cells were analyzed or sorted by flow cytometry using a FACSTAR®. Data analysis was performed using the CELLQuest software (Becton Dickinson, San Jose, CA).

Antibody and Complement Depletion. To deplete $CD4^+$ cells, spleen cells were incubated with anti-CD4 (GK1.5) for 45 min on ice, washed once with RPMI 1640, and then incubated with MAR 18.5 for 45 min on ice. The cells were washed once with RPMI 1640, treated with rabbit complement H2 (Pel-Freez Clinical Systems, Brown Deer, WI), and then incubated at 37°C in a humidified 5% CO_2 incubator for 45 min. At the end of the incubation, the cells were washed three times with RPMI 1640.

Target Cell Preparation. MC57G ($H\text{-}2^b$), a methylcholanthrene-induced fibroblast cell line from C57BL/6 mice, was propagated in MEM (GIBCO BRL, Gaithersburg, MD) supplemented with 100 U/ml of penicillin G, 100 μg/ml streptomycin sulfate, 2 mM l-glutamine, 10 mM Hepes (United States Biochemical Corp., Cleveland, OH), and 10% heat-inactivated (56°C, 30 min) fetal bovine serum (Sigma Chemical Co.). The TAP-2–deficient cell line RMA-S ($H\text{-}2^b$) was from Hans-Gustaff Ljunggren (Karolinska Institute; Stockholm, Sweden) and was grown in RPMI 1640, supplemented as above. To prepare target cells, MC57G cells were infected with LCMV or PV at a multiplicity of infection of 0.1 PFU/cell and incubated for 2 d at 37°C. RMA-S cells were pulsed overnight with 200 μM of LCMV peptide glycoprotein 33 (GP33), GP276, or nucleoprotein 396 (NP396), as described previously (20).

Cytotoxicity Assays. Cell-mediated cytotoxicity was determined by using a standard microcytotoxicity assay (21). In brief, target cells were pelleted and resuspended in 100 μCi of $Na^{51}Cr$ (DuPont-NEN, Boston, MA) per 10^6 cells and incubated at 37°C in a humidified 5% CO_2 incubator for 1 h. They were washed three times with media, resuspended to 5×10^4/ml, and 0.1 ml was added to round-bottomed microtiter wells (Falcon Labware, Becton Dickinson & Co., Oxnard, CA). Varying numbers of effector cells were added in 0.1-ml vol to achieve the desired E/T ratios. For a spontaneous ^{51}Cr-release control, 0.1 ml of media was substituted for effector cells. Maximum release was determined by adding 0.1 ml of 1% NP-40 (United States Biochemical Corp.) to the target cells. After 6 h at 37°C, the plates were centrifuged at 200 *g* for 5 min, and 0.1 ml of supernatant was removed from each well and counted on a gamma counter (model 5000; Beckman Instruments Inc., Palo Alto, CA). Data were presented as: *percent specific ^{51}Cr-release* $= 100 \times$ [(*experimental cpm* − *spontaneous cpm*)/(*maximum release cpm* − *spontaneous cpm*)].

Oligonucleotides and Labeling. The Vβ8.1, Vβ8.2, Cβ, and Jβ primer sequences were derived from a previous report by Pannetier et al. (22). Vβ8.1 and Cβ primers used for RT-PCR reactions and unlabeled Jβ primers were synthesized by BioSynthesis (Lewisville, TX). For ^{33}P-labeling, Jβ primers were labeled by using T4-polynucleotide kinase (Boehringer Mannheim, Mannheim, Germany) and [γ-^{33}P]ATP (DuPont-NEN). Fluorescent Jβ primers were synthesized and labeled at the 5′ end with fluorophores (6-Fam, Hex, or Ned) by PE (Applied Biosystems, Inc., Foster City, CA). These fluorescent dye–labeled oligonucleotides were purified by high performance liquid chromatography by the manufacturer to remove the unlabeled oligonucleotides and unreacted dyes.

RNA Extraction. Total RNA was extracted from spleen cells, peritoneal exudate cells (PEC), and peripheral blood (PB) by the acid-guanidinium thiocyanate-phenol-chloroform method (23). In brief, $<10^7$ spleen cells or PEC were pelleted and subsequently extracted with 0.5 ml of solution D (4 M guanidinium thiocyanate, 25 mM sodium citrate, 0.5% sarcosyl, and 1% 2-mercaptoethanol) (Sigma Chemical Co.), 50 μl of 2 M sodium acetate, pH 4 (Sigma Chemical Co.), 0.5 ml phenol, pH 8 (United States Biochemical Corp.), and 0.1 ml chloroform (EM Science, Gibbstown, NJ)/isoamyl alcohol (Fisher Scientific Co.) (49:1). After a 15-min incubation on ice, the reaction mixture was centrifuged at 10,000 *g* for 20 min. The aqueous phase was transferred and subjected to two cycles of precipitation with 2-propanol (Fisher Scientific Co.). For PB samples, 0.25 ml PB (without anticoagulant) was mixed with 0.5 ml solution D and 75 μl 2 M sodium acetate and subjected to RNA extraction as described above. When RNA was extracted from a small amount of lymphocytes such as PB RNA samples were washed twice with 70% ethanol after propanol precipitation to remove excess salt, which otherwise would inhibit the RT-PCR reaction.

CDR3 Length Spectratyping. RNA samples, equivalent to $5\text{–}10 \times 10^5$ cells or 0.12 ml of blood, were amplified by using a GeneAmp RNA PCR kit (Perkin-Elmer Corp., Branchburg, NJ) with Vβ8.1 and Cβ primers, according to the manufacturer's instructions. The amplification started with a denaturing step of 1 min at 94°C, followed by 40 cycles consisting of 1 min at 94°C, 1 min at 55°C, and 1 min at 72°C, and a 5-min incubation at 72°C to complete the product extension. Although our primer sequences were derived from those published by Pannetier et al. (22), our PCR cycle profile was modified to optimize the amplification of PB samples. Nevertheless, the CDR3 spectratype remained the same when splenic RNA was amplified by either condition. To determine whether lowering the annealing temperature to 55°C would cause a cross-reaction with the Vβ8.2 sequence, the splenic RNA of an HY transgenic mouse (24), which expresses the Vβ8.2 transgene in all T cells, was tested. Some cross-reaction did occur when samples were amplified at the 55°C or 60°C annealing temperature, but this cross-reaction at the 55°C annealing temperature contributed to <3% of the Vβ8.1 message during the acute LCMV infection.

2 μl of the amplified PCR products was subjected to either one cycle of run-off with radiolabeled Jβ primers or five cycles of run-off with fluorophore-labeled Jβ primers in a final volume of 10 μl reaction mixture containing 50 mM KCl, 10 mM Tris-HCl, pH 8.3, 1 mM $MgCl_2$, 200 μM dNTP, 0.25 U *Taq* polymerase (Perkin-Elmer Corp.), and 0.1 μM of labeled Jβ primers. 2 μl of the radioactive products was mixed with equal volumes of gel-loading buffer (95% formamide, 20 mM EDTA, 0.05% bromophenol blue, 0.05% xylene cyanol FF) and loaded on 5% Long Ranger sequencing gels (FMC Bioproducts, Rockland, ME); 1 μl of the fluorescent products was mixed with an equal volume of gel-loading buffer (5 parts of 100% formamide and 1 part of 2.5% blue dextran/50 mM EDTA) and loaded onto a 4.75% acrylamide sequencing gel. For radioactive products, the gels were exposed to a phosphor screen, and the radioactive intensity of each band was quantified by a PhosphorImager (Molecular Dynamics, Sunnyvale, CA). For fluorescent products, the results were analyzed on an automated DNA sequencer using GeneScan software (Perkin-Elmer Applied Biosystems, Emeryville, CA). Both radiolabeled and fluorescent-labeled methods gave comparable results. However, the fluorescent-labeled method was easier and more efficient because fluorescent-labeled primers are stable and run-off products labeled with three different fluorescent dyes can be analyzed in the same gel lane. Therefore, we changed our technique from the radiolabeled method to fluorescent-labeled method in the middle of our study, when the fluorescent-labeled method became available at our institution.

Direct Sequencing of PCR Products. RT-PCR products in 30–75 μl were purified by using a QIAquick PCR purification kit

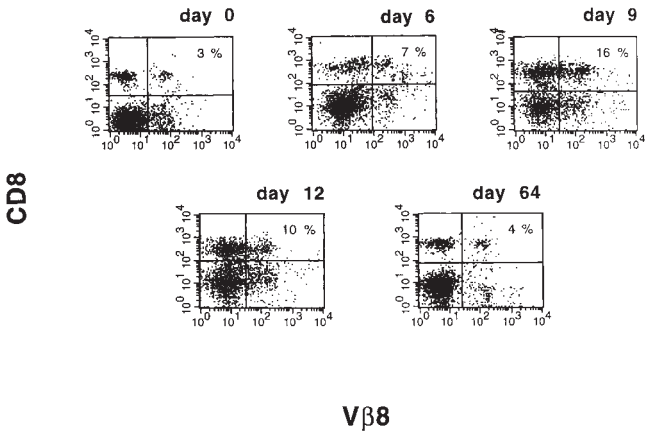

Figure 1. Vigorous expansion of $CD8^+V\beta8^+$ cells during acute LCMV infection. 6–8-wk-old C57BL/6 mice were inoculated intraperitoneally with 4×10^4 PFU of LCMV. Spleen cells were harvested at various time points after LCMV infection, and stained with anti-CD8 PE and anti-Vβ8.1/8.2 FITC, and analyzed by flow cytometry. Cell percentages for quadrants (clockwise from upper left) were: (*day 0*) 12, 3, 10, 75; (*day 6*) 13, 7, 8, 72; (*day 9*) 35, 16, 13, 36; (*day 12*) 25, 10, 14, 51; and (*day 64*) 13, 4, 8, 75.

(QIAGEN Inc., Santa Clarita, CA) and subjected to DNA sequencing by using specific unlabeled Jβ primer and a Dye Terminator Cycle Sequencing kit (Perkin-Elmer, Foster City, CA). The sequencing products were run through 4.75% sequencing gels and analyzed on an automatic DNA sequencer (model 373; PE Applied Biosystems).

Statistical Analysis. To determine the significance of the preservation of a dominant peak in the memory response, we compared the proportion of the peak within that specific Jβ spectratype in the immune mouse with that of a comparable peak in naive mice. Because the naive spectratypes invariably have a normal Gaussian distribution, the mean and standard deviations of the peak within a certain Jβ spectratype were calculated from five naive mice. The preservation of a significant dominant peak in memory was defined as those peaks whose proportions exceeded the mean of naive mice by >2 SD.

Results

Vβ8 Usage in LCMV Infection. To study the evolution of TCR repertoire usage in LCMV infection, we chose to analyze the Vβ8 TCR, because it is expressed on a significant number of T cells in the C57BL/6 mouse (4), and because the LCMV-specific lysis is highly represented within the Vβ8 population (19). As shown in Fig. 1, acute LCMV infection expanded the $CD8^+V\beta8^+$ cells from 3 to 16% of spleen cells or from 20 to 30–35% of total $CD8^+$ cells. Therefore, the $CD8^+V\beta8^+$ cells contributed greatly to the major expansion of the $CD8^+$ population during acute LCMV infection. To characterize the specificity of these $CD8^+V\beta8^+$ cells, we tested their cytolytic activities against targets infected with LCMV or with the heterologous virus, PV. As shown in Table 1, the $CD8^+V\beta8^+$ cells induced during the acute LCMV infection specifically lysed LCMV-infected but not PV-infected targets. The $CD8^+V\beta8^+$ cells also specifically lysed RMA-S cells pulsed with LCMV peptides GP33, GP276, and NP396. We have reported previously that RMA-S cells pulsed with peptides from other viruses are lysed much less by LCMV-induced T cells (20). Interestingly, enrichment of specific CTL activities against all three LCMV immunodominant epitopes was detected within the $CD8^+V\beta8^+$ cells, indicating that this subset of T cells is useful for examining the dynamics of

Table 1. *Enrichment within the $CD8^+V\beta8^+$ Population of Specific CTL Activity against 3 LCMV Immunodominant Epitopes*

		% Specific lysis								
		Effector cells (E/T ratio)*								
		$CD8^+V\beta8^+$			$CD8^+V\beta8^-$			Unsorted		
EXPT	Targets	20	10	5	20	10	5	100	50	25
1.	LCMV-infected MC57G	51	32	26	36	28	17	60	59	40
	PV-infected MC57G	2	3	1	1	1	−1	−2	−2	−4
	MC57G	2	1	−1	−1	−4	−3	−2	−2	−2
2.	GP33-pulsed RMA-S	89	70	57	75	62	49	91	75	51
	GP276-pulsed RMA-S	70	61	45	55	39	28	83	62	41
	NP396-pulsed RMA-S	98	90	74	70	67	49	98	88	70
	RMA-S	0	0	−2	0	0	−2	1	−1	0

Specific lysis mediated by each population of T cells against infected or peptide-coated targets was determined in a 6-h ^{51}Cr-release assay. Spleen cells from C57BL/6 mice at 9 d after infection with LCMV were sorted by FACS® to obtain $CD8^+V\beta8^+$ cells. The purities of the sorted $CD8^+V\beta8^+$ and $CD8^+V\beta8^-$ cells in EXPT 1 were 85 and 98%, and those in EXPT 2 were 90 and 98%, respectively.
*The numbers under each effector cell type represent the effector to target ratio used.

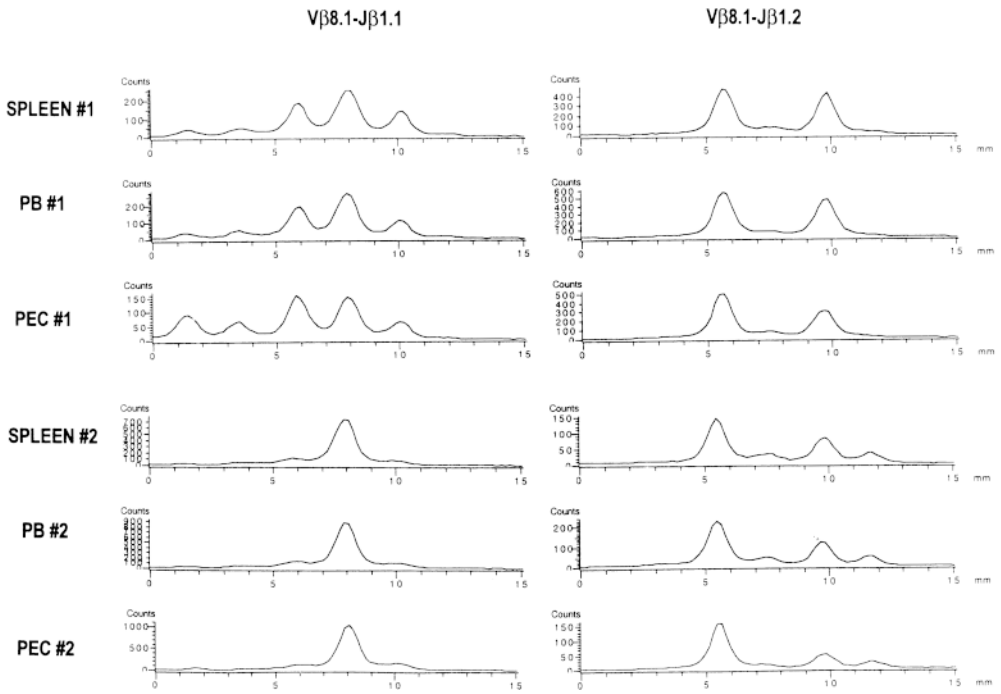

Figure 2. Similar CDR3 profiles of the Vβ8.1-Jβ run-off products from acute LCMV-infected spleen, PB, and PEC within a mouse. Total RNAs were extracted from spleen leukocytes, PB, and PEC 8 d after LCMV infection and subjected to spectratyping as described in Materials and Methods. Radioactivity intensity (*y-axis*) was plotted against relative CDR3 size (*x-axis*).

a complex T cell response directed against several epitopes (Table 1).

We next examined the contribution of the Vβ8.1 and 8.2 subsets to the expansion of the Vβ8 population during acute LCMV infection by using RT-PCR with the Vβ8.1- and 8.2-specific primers in combination with the Cβ primer. A much stronger band was detected when the acute LCMV-infected splenic RNA was amplified with the Vβ8.1 and Cβ primers (data not shown). Thus, analysis of the Vβ8.1 TCR usage would shed light on the evolution of a significant part of the LCMV-induced T cell repertoire.

Similar Spectratypes Are Detected in Spleen, PB, and PEC within an Individual Mouse. To determine the LCMV-induced Vβ8.1 TCR repertoire usage directly ex vivo, we analyzed the TCR usage by CDR3 length spectratyping. Pilot experiments were performed by using five Jβ primers to determine the spectratype during acute LCMV infection. Whereas naive mice generated the typical Gaussian distribution (see Fig. 5, *day 0*), spectratypes were skewed in LCMV-infected mice (Figs. 2 and 3). The LCMV-induced splenic spectratypes were different among individual mice, although there were some similarities. To confirm that the variation between spectratypes was due to the differences of TCR usage among individual mice instead of problems with the reproducibility of the technique, we took two different RNA samples and performed spectratyping in triplicates, beginning with separate RT-PCR reactions. The spectratypes were highly reproducible within each RNA sample (data not shown).

Because the spectratypes varied between individual mice, studies on the evolution of the repertoire necessitated following the same individual mice longitudinally during

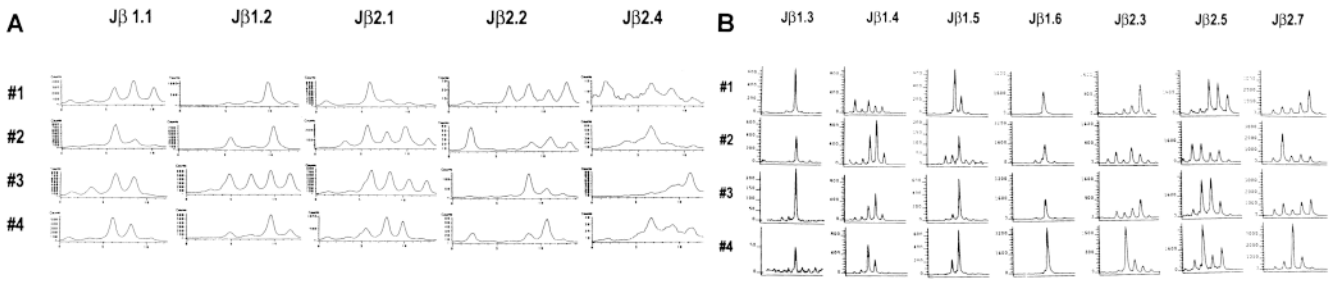

Figure 3. Host diversity in the broad spectrum of Vβ8.1$^+$ T cell response as demonstrated by complete CDR3 size analysis within the Vβ8.1$^+$ cells from day 8 LCMV-infected mice. CDR3 size patterns were obtained from day 8 LCMV-infected PBL from four C57BL/6 mice. Total RNAs from the PB were extracted and subjected to spectratyping as described in Materials and Methods. The PCR products were subjected to run-off reactions using [γ-^{33}P]ATP-labeled (*A*) or fluorescent (*B*) Jβ primers. Jβ1.3 and Jβ1.6 were labeled with the fluorescent dye Ned; Jβ1.4 and Jβ2.5 with 6-Fam; Jβ1.5, Jβ2.3, and Jβ2.7 with Hex. Because primers labeled with different fluorophores give different fluorescent intensity, it is not appropriate to compare the relative fluorescent intensity between different fluorophore-labeled run-off products. The magnitude of fluorescent intensities is 6-Fam > Hex > Ned.

LCMV infection, as a comparison of spectratypes between the mice would be impossible to interpret. This could only be done by examining PB spectratypes, as examining spleen cell spectratypes would require killing the mice. To see whether the PB spectratypes were representative of those in other immunological compartments, we compared the spectratypes in spleen, PB, and PEC after LCMV infection and found them to be nearly identical (Fig. 2). Fig. 2 shows the spectratypes for day 8 after infection, and spectratypes similar for spleen, PB, and PEC were also observed at days 6 and 12 after infection (data not shown). Thus, it was feasible to study the evolution of TCR repertoire usage in LCMV infection by determining the PB spectratype.

Acute LCMV Infection Expands a Broad Spectrum of Vβ8.1$^+$ T Cells. To examine the complete Vβ8.1$^+$ T cell repertoire in acute LCMV infection, we analyzed the Vβ8.1 spectratypes with primers specific to all 12 Jβs. The Vβ8.1 spectratypes from naive mice at 6 wk and 4 mo of age invariably had a normal Gaussian distribution for each of the Jβs (data not shown). In contrast, the acute LCMV infection expanded a broad spectrum of Vβ8.1$^+$ T cells. Dominant peaks were consistently detected in the spectratypes of Jβs 1.1, 1.2, 1.3, 1.5, and 1.6 in most of the mice tested; some other peaks occasionally were detected in the Jβ2s (Fig. 3; The two types of graphic displays reflect the fact that some analyses used ^{33}P-labeling [Fig. 3 *A*] and others, done later in the study, used fluorescent labeling [Fig. 3 *B*]). The spectratypes determined by Jβs 2.2 and 2.4 were consistently very weak, as the radioactivity intensities (Y-axes) were low in both acutely infected and naive mice. Thus, genetically identical hosts generate somewhat predictable but nevertheless different T cell spectratypes in response to the same virus. Of the 12 Jβs, Jβ1s were preferentially used. This preferential expansion was elicited by the virus infection and not by the diluted culture media vehicle, as the spectratype from vehicle-injected mice had a normal Gaussian distribution (data not shown). The Vβ8.1 spectratype in acute PV infection, which also activated Vβ8$^+$ T cells, although to a lesser extent, was unlike that observed in the acute LCMV infection, as PV infection did not generate consistent dominant peaks in the spectratypes of Vβ8.1-Jβ1.1 and Vβ8.1-Jβ1.2 (data not shown). The observation of discrete LCMV-induced clonal expansion by spectratyping indicates that the massive proliferation of T cells within the Vβ8.1 population is unlikely due to LCMV-encoded superantigen stimulation or nonspecific cytokine stimulation.

The Skewed Vβ8.1 Spectratype Is Dominated by the CD8$^+$ T Cell Population. To evaluate the contribution of the CD4$^+$ and CD8$^+$ T cell populations to the skewed Vβ8.1 spectratype during acute LCMV infection, we depleted CD4$^+$ T cells from the spleen cells at 9 d after LCMV infection and compared the spectratype of the CD4-depleted spleen cells to that of the total spleen cells. As shown in Fig. 4, experiment 1 (*EXPT. 1*), the spectratype of the CD4-depleted spleen cells was very similar to that of the total spleen cells, indicating that CD4$^+$ T cells contribute little

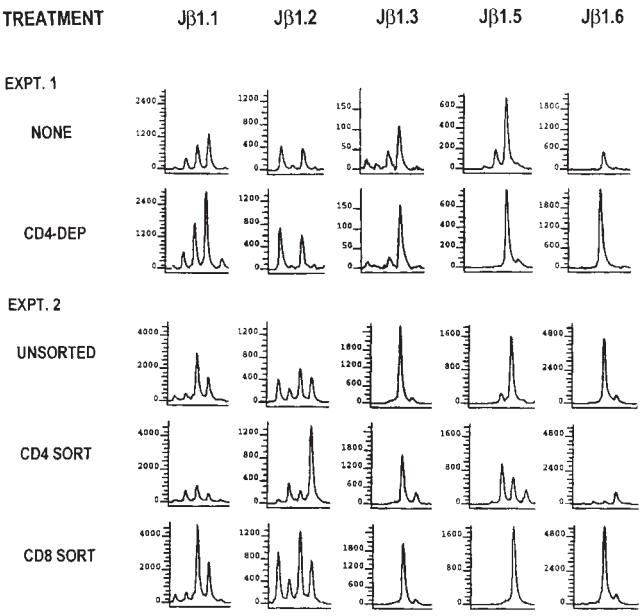

Figure 4. Skewed Vβ8.1 spectratypes within CD8$^+$ T cells during acute LCMV infection. (*EXPT. 1*) Spleen cells from a C57BL/6 mouse at 9 d after LCMV infection were depleted of CD4$^+$ T cells as described in Materials and Methods. 0.5% of CD4$^+$ T cells were left after CD4 depletion. (*EXPT. 2*) Spleen cells from a C57BL/6 mouse at 8 d after LCMV infection were sorted by FACS® to obtain CD4$^+$ or CD8$^+$ T cells. The purities of the sorted CD4$^+$ or CD8$^+$ T cells were 98 and 99%, respectively. Total RNA was extracted from each population of T cells and subjected to spectratyping.

to the skewed Vβ8.1 spectratype. We also sorted CD4$^+$ and CD8$^+$ T cells from the spleen cells at 8 d after LCMV infection and determined their Vβ8.1 spectratype. The CD8 spectratype was nearly identical to that of the unsorted spectratype (Fig. 4, *EXPT. 2*). Even though responses could be seen within the Jβ1.2 and Jβ1.3 CD4 spectra, in the total T cell population they were not sufficient to influence the more dominant response associated with the CD8$^+$ cells. Taken together, the skewed Vβ8.1 spectratype is dominated by the CD8$^+$ T cell population, and studies of the LCMV-induced Vβ8.1 spectratype by using PB or spleen reflect mainly the LCMV-induced CD8 spectratype.

The Vβ8.1 Spectratype Changes Little during the Apoptosis Phase of the T Cell Response. The fact that LCMV-induced spectratypes differed between individual mice indicated that studies on the evolution of the T cell response could not be done by comparison of one mouse to another, but instead required longitudinal studies within the same mouse. We were able to do this by examining PB spectratypes. From days 10 to 14 after infection, a time period immediately after the peak in the massive CD8$^+$ T cell proliferation, the majority of the T cells undergo apoptosis in vivo (11). Most virus is cleared by ~7 d after infection, and we asked whether there is a further selection of T cell receptors after viral clearance and during this apoptosis phase. Fig. 5 shows the PB spectratype from individual mice at days 6 to 12 after infection and compares it with

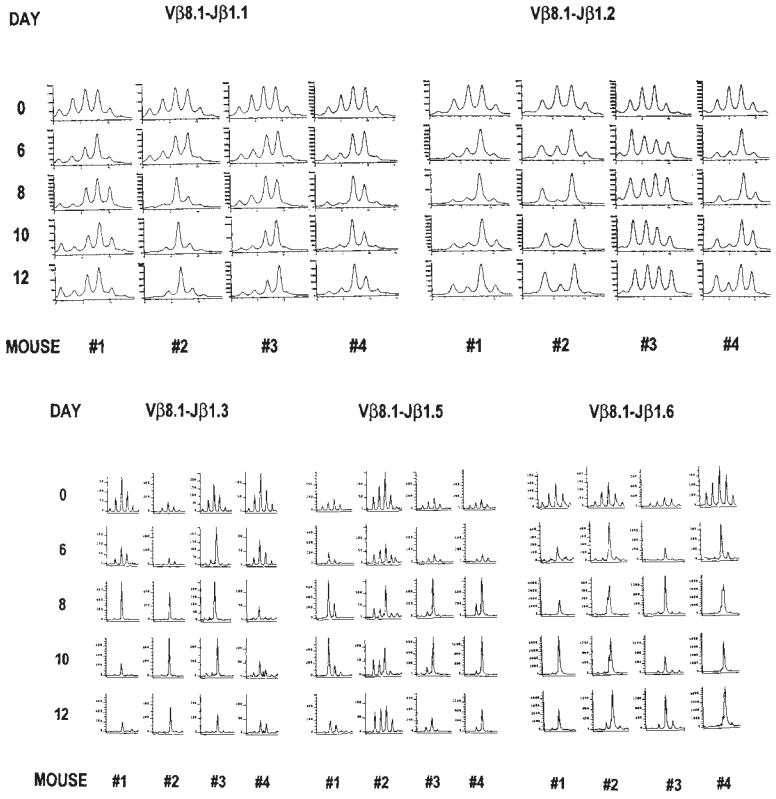

Figure 5. Preservation of Vβ8.1 spectratypes during the T cell apoptosis phase from days 8 to 12 after LCMV infection. The representative CDR3 profiles from the PB of four acutely LCMV-infected mice 6–12 d after infection are displayed. Since the naive spectratypes invariably have a normal Gaussian distribution, we plot at the top of each column day 0 spectratypes from two naive control mice. To avoid traumatizing the mice at the time of LCMV infection, day 0 samples were not taken from the same mice analyzed on the subsequent days. The PCR products were subjected to run-off reactions using [γ-^{33}P]ATP-labeled (Jβ1.1 and Jβ1.2) or fluorescent (Jβ1.3, Jβ1.5, and Jβ1.6) Jβ primers.

the normal Gaussian distribution pattern of separately examined uninfected mice. The naive spectratype began to change by day 5 (data not shown) and evolved into a distinct spectratype by day 8 after infection. This distinct spectratype remained stable from days 8 to 12 after infection, even though there was a significant decrease in the number of T cells after day 9. This suggests that after viral antigens are cleared, further selection of the T cell repertoire does not occur during the T cell apoptosis period.

Sequence Analyses Show Stability of the TCR Repertoire within an Individual Mouse but Distinctions among Mice. To determine whether a discrete spectratype peak was predominantly monoclonal and whether a further selection of the TCR sequences occurred from days 8 to 12 after LCMV infection, we directly sequenced PCR DNA amplified from day 8 and day 12 LCMV-infected PBL (Fig. 5) by using Jβ primers that had revealed singular and dominant spectratype bands. Fig. 6 shows that this technique revealed predominantly monoclonal TCR sequences in some mice. The sequences of mouse 4 were monoclonal, whereas the sequences in mice 1 and 3 each appeared to reveal two clones. The sequences in the CDR3 region remained unchanged from days 8 to 12 after LCMV infection in mice 1, 3, and 4. In mouse 2, it was hard to draw any conclusion by comparing the sequences between day 8 and day 12 of LCMV infection because too many unreadable sequences were present in the CDR3 region, indicating that several clones were present. Surprisingly, the DNA sequences were very different among these four mice even though they had a very similar Jβ1.6 spectratype with discrete, similarly sized bands. Notably, a conserved GXXN amino acid motif with a non-V, non-J–encoded glycine residue at position 96 was detected in all the sequences analyzed, even those from the multiclonal mouse 2, suggesting the importance of this motif for the recognition of LCMV. These DNA sequence data further support the concepts that genetically identical hosts generate different

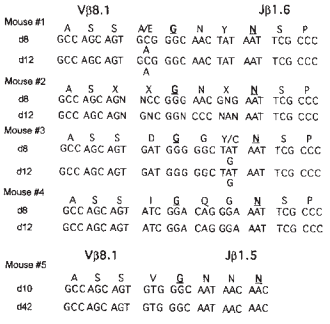

Figure 6. Stability of TCR sequences after viral clearance. DNA sequences and deduced amino acid sequences of the Vβ8.1-Jβ1.6 and Vβ8.1-Jβ1.5 were derived from direct sequencing of PCR DNA. The sequences shown represent the deduced amino acid sequences of the VDJ junctions beginning with residue 92 (33) of the amplified PCR products that were rearranged to the Jβ1.5 and Jβ1.6 gene segments. PCR products were amplified from the same individual mice at various time points after LCMV infection and then subjected to spectratyping. Discrete spectratype peaks were selected for direct DNA sequencing as described in Materials and Methods. The d8 and d12 DNA sequences from mice 1–4 were derived by using the same PCR products used for spectratyping in Fig. 5. At some positions it was clear from the DNA sequence data that either of two amino acids were encoded by what were probably two clones, and these are designated in the A/B format. The unreadable DNA sequences and amino acid translation in mouse 2 were designated *N* and *X*, respectively.

T cell responses to the same antigen and that after 7 d of LCMV infection, when virus is cleared, no further selection of the T cell repertoire occurs.

The Vβ8.1 Spectratype Changes Continuously from 7 to 13 d under Conditions of Clonal Exhaustion by High Doses of LCMV Clone 13 Infection. A high dose LCMV clone 13 infection results in a transient antiviral CTL response followed by clonal exhaustion of the virus-specific T cells, due to the overwhelming amount of antigen present (7). We asked how global the T cell exhaustion was by examining the Vβ8.1 spectratype. As shown in Fig. 7 *A*, the spectratype changed continuously from 7 to 13 d after LCMV clone 13 infection, when excess viral antigens were present. Some dominant peaks in the Vβ8.1 spectratype disappeared at days 10 or 13 after infection: mouse 1 Jβ1.1, mouse 3 Jβ1.2, mouse 4 Jβ1.3, mice 1 and 4 Jβ1.5, and mouse 3 Jβ1.6. Others changed from 7 to 13 d after infection, accompanied with new peak formation: mouse 2 Jβ1.1, and mice 2 and 4 Jβ1.6. However, others remained stable, such as those of mice 1 and 4 Jβ1.2, mouse 3 Jβ1.3, and mouse 1 Jβ1.6. To determine whether all of the virus-induced $CD8^+$ T cells were clonally exhausted and whether the skewed spectratype was due exclusively to $CD4^+$ T cells, we sorted $CD4^+$ and $CD8^+$ cells from the spleen cells at 13 d after LCMV clone 13 infection to determine their Vβ8.1 spectratype. As shown in Fig. 8, skewed spectratypes were detected in both $CD4^+$ and $CD8^+$ T cell populations. Therefore, the change of spectratype from 7–13 d after LCMV clone 13 infection was not due to selective preservation of the $CD4^+$ T cell population.

To investigate whether a subset of T cells activated by high dose clone 13 infection was resistant to clonal exhaustion and survived in persistent infection, we examined the Vβ8.1 spectratype during longer term infections. Although we still detected skewed Vβ8.1 spectratypes at day 15 and, to a lesser extent, at day 22 after infection (data not shown), almost all of the spectratypes became like those of naive mice by 42 d after infection and remained the same thereafter (Fig. 7 *B*). Only very weak non-Gaussian spectratypes could sometimes be detected, such as that of Jβ1.6 in mouse 5 (Fig. 7 *B*). This observation suggests that most clone 13–induced T cells eventually underwent clonal exhaustion. In summary, these results support the concept that continuous selection of T cells occurs in the presence of persistent antigens, but they also show that T cell clonal exhaustion occurs in the great majority of the virus-induced T cells, and only very weak T cell responses can be detected long after infection.

The LCMV-immune Spectratype Is Different from the Naive Spectratype but Resembles That of Acute Infection. It has not been known which activated T cells and what proportions of these T cells survive the apoptosis phase and become memory cells. Our LDA data indicate that there is only a twofold reduction in the numbers of LCMV-specific pCTL per $CD8^+$ cell between the peak of the acute infection and long term memory. The efficiencies of these assays, which indicate that ~2% of the $CD8^+$ T cells are precursors for LCMV-specific CTL in immune mice, are unknown, and a much higher proportion of the T cells in the immune

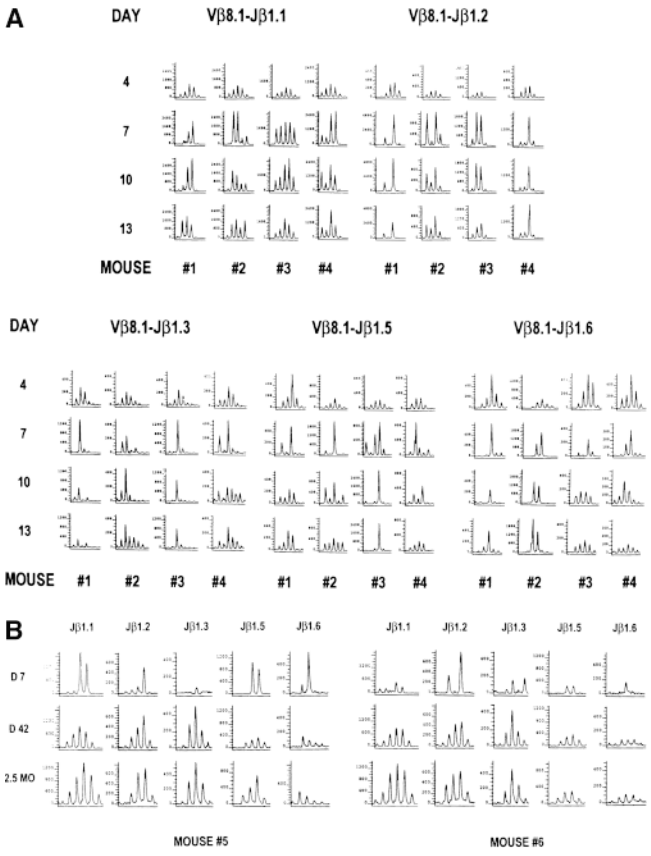

Figure 7. Evolution of the Vβ8.1 spectratypes under conditions of clonal exhaustion by high doses of LCMV clone 13 infection. (*A*) Continuous change from days 7 to 13 in Vβ8.1 spectratypes was detected in high dose LCMV clone 13 infection. The representative CDR3 profiles from the PB of four LCMV clone 13–infected mice are displayed. (*B*) Loss of skewed Vβ8.1 spectratypes was detected after long term clone 13 infection. The representative CDR3 profiles from the PB of two LCMV clone 13–infected mice are displayed. The PCR products were subjected to run-off reactions using fluorescent Jβ primers.

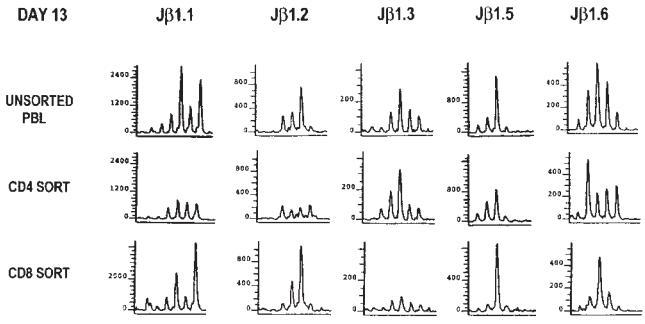

Figure 8. Skewed Vβ8.1 spectratype within $CD8^+$ T cells under conditions of clonal exhaustion by high dose LCMV clone 13 infection. The representative CDR3 profiles were obtained from PB and sorted spleen cells at 13 d after LCMV clone 13 infection. The spleen cells were sorted by FACS® to obtain $CD4^+$ and $CD8^+$ T cells. The purities of the sorted $CD4^+$ and $CD8^+$ T cells were 88 and 95%, respectively. Total RNA was extracted from each population of T cells and subjected to spectratyping.

state may be specific for the virus than previously thought. A recent study on tetrameric MHC–peptide staining of TCR supports the concept that a substantial number of memory cells remain virus specific (13). To determine the preservation and distribution of virus-induced T cell species in the memory state, we compared the Vβ8.1 spectratype in the acute LCMV infection with that in the immune state from the same individual mice. The immune spectratype (Fig. 9 *A*, day 42; Fig. 9 *C*, 2–2.5 mo) was very different from the naive spectratype but resembled a combination of that of acutely infected and naive mice, consistent with only a moderate dilution of memory cells with naive cells (Fig. 9 *A*). This supports the concept that LCMV infection alters the host T cell repertoire dramatically and leaves it with a high frequency of LCMV-specific T cells (9). We found that very dominant peaks in the acute infection often remained present in the immune state. Six dominant peaks consisting of ~70% of the T cells in their specific Jβ spectratypes were selected for sequence analysis. By direct sequencing of the PCR DNA, we were able to resolve a monoclonal sequence from one of the six peaks. Its TCR sequence was identical to that seen at day 10 of the acute infection (Fig. 6), and, notably, it had the same GXXN conserved motif seen in the acute Jβ1.6 samples. It appears that very strong dominant peaks in the acute infection, regardless of which Jβ they use, can be detected in the immune state by spectratyping.

Although pCTL data have shown that a high frequency of LCMV-specific pCTL remains stable throughout the lifetime of the mouse (1), it was still not clear how the TCR repertoire evolved long after infection and whether such a high frequency of pCTL reflected a drastic alteration of the host T cell repertoire in long term memory. Therefore, we examined the evolution of Vβ8.1 TCR repertoire into long term memory by spectratyping. As shown in Fig. 9 *B*, dominant peaks were stably preserved from acute LCMV infection through 7 mo after infection, and during this period of time no other new peaks were generated.

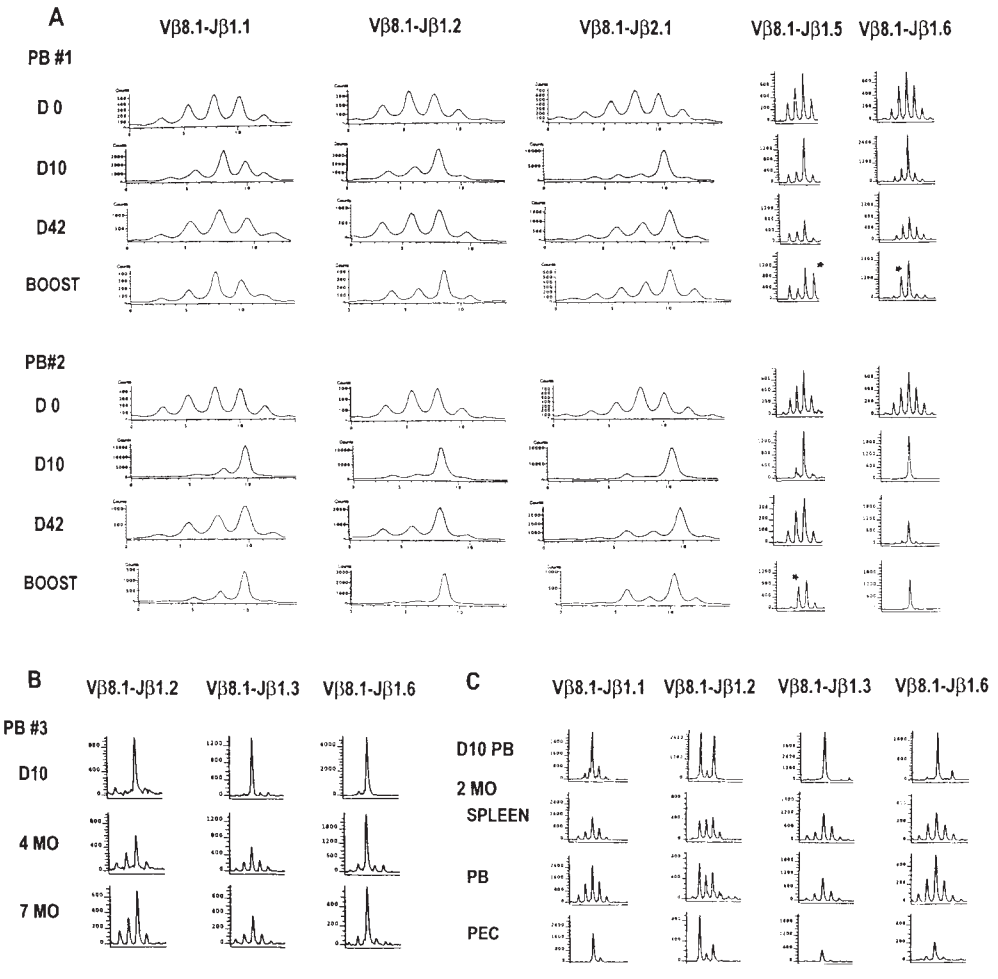

Figure 9. Evolution of the Vβ8.1 spectratypes from primary LCMV infection into memory and secondary responses. (*A*) The LCMV-immune Vβ8.1 spectratype resembled that of acute infection, and most of the primary spectratypes were preserved during secondary infection. CDR3 profiles were obtained from PB of two individual mice at days 10 (*D10*) and 42 (*D42*) after primary LCMV infection and at day 5 after secondary infection. Day 0 spectratypes were obtained from two different naive controls. The run-off reactions were primed with radiolabeled (*Jβ1.1*, *Jβ1.2*, and *Jβ2.1*) or fluorescent (*Jβ1.5* and *Jβ1.6*) Jβ primers. The significance of the preservation of dominant peaks in the immune state was determined as described in Materials and Methods. In this figure, all of the dominant peaks except those of Jβ1.1, Jβ1.2, and Jβ1.6 from PB 1 remained skewed in memory. In secondary infection, some newly formed peaks such as those of Jβ1.5 in PB 1 and PB 2, and Jβ1.6 in PB 1 are marked with asterisks. (*B*) Dominant peaks were preserved from acute LCMV infection into long term memory. Representative CDR3 profiles were obtained from PB of one mouse at day 10 (*D10*), 4 mo (*4MO*), and 7 mo (*7MO*) after LCMV infection. In this figure, the Jβ1.2 and Jβ1.6 spectratypes were significantly preserved into 7 mo after infection. (*C*) Skewed Vβ8.1 spectratypes were detected in LCMV-immune PEC. CDR3 profiles were obtained from PB of acutely LCMV-infected and from LCMV-immune spleen leukocytes, PB, and PEC. Total RNA was extracted from PB of day 10 (*D10 PB*) LCMV-infected mice and from LCMV-immune spleen leukocytes (*SPLEEN*), PB (*PB*), and PEC (*PEC*) of two immune mice at 2–2.5 mo (*2MO*) after LCMV infection. The run-off reactions were primed with fluorescent Jβ primers. The spectratypes were obtained from two different mice.

Thus, a high frequency of LCMV-induced T cells can be preserved from acute infection into long term memory and permanently skew the host T cell repertoire.

In the immune state, the spectratypes of PB and spleen were similar to each other, but that of PEC was somewhat different (Fig. 9 *C*) in that it even more closely resembled that of the PB during the acute infection, which is consistent with our previous findings that LCMV-immune PEC contain a higher frequency of LCMV-specific pCTL (25). This might be because the LCMV infection had been established previously by i.p. inoculation or because few naive T cells accumulate in the peritoneal cavity to dilute out the memory cell population.

To determine the effects of secondary LCMV infection on the spectratype, we rechallenged the immune mice with a high dose of LCMV (10^7 PFU) and then analyzed their Vβ8.1 spectratypes. The LCMV-induced secondary spectratype was similar in most of the dominant peaks but was different in some, compared with that of the primary infection. Fig. 9 *A* shows that subdominant peaks, such as those of Jβ1.5 in mice 1 and 2 and that of Jβ1.6 in mouse 1, appeared in the secondary response for the first time. The further selection of the TCR repertoire was not due to a nonspecific activation induced by culture media, as the media-injected LCMV-immune mice had a spectratype similar to that of their immune state (data not shown). To confirm that the secondary infection activated LCMV-specific T cells, we examined CTL activities on the same day (day 5) as the spectratype analyses after secondary LCMV infection. Significant LCMV-specific CTL activities were detected (63% specific lysis against LCMV-infected targets at E/T = 200 in a direct ex vivo 6-h assay). These results support the generally accepted concept that further maturation of the T cell response can occur in a secondary viral infection.

Discussion

In this study we have provided evidence supporting the concepts that (*a*) the virus-induced T cell repertoire during a primary infection changes little after clearance of the viral antigens; (*b*) it is continuously selected in the presence of excess viral antigens leading to persistent infection; (*c*) the LCMV infection substantially skews the host T cell repertoire in the memory state long after virus is cleared; and (*d*) genetically identical mice generate somewhat predictable but nevertheless remarkably different T cell responses to the same antigens. Evidence supporting the first and second concepts is that the LCMV-induced Vβ8.1 spectratype changes little between 8 and 12 d after LCMV infection, a time when the virus has already been cleared (Fig. 5), but it continues to evolve from 7 to 13 d after the infection of a high dose of the clonally exhausting LCMV clone 13 (Fig. 7 *A*). Our spectratype data are consistent with our kinetic studies on the pCTL frequencies, which show that the proportions of the three LCMV immunodominant peptide–specific pCTL become fixed within the LCMV-specific repertoire by day 7 after infection, and thereafter remain the same throughout the lifetime of the mouse (9). Although a limitation of the spectratyping technique is that it cannot detect subtle changes of the TCR usage within each peak of the spectratype, our direct sequencing of the PCR DNA revealed that the TCR sequences of the same-sized dominant peaks within a specific Jβ spectrum induced by the parent LCMV strain remained stable between days 8 and 12 after infection (Fig. 6). In contrast, the spectratype analyses showed that from 7 to 13 d after LCMV clone 13 infection the spectratypes changed continuously (Fig. 7 *A*); such changes were not due to selective preservation of $CD4^+$ T cells, as skewed spectratypes were detected in both $CD4^+$ and $CD8^+$ T cell populations at 13 d after infection (Fig. 8). The disappearance of the dominant peaks from 7 to 10 d of the clone 13 infection paralleled the deletion of the virus-specific CTL precursors; such a reduction in pCTL was originally reported by Moskophidis et al. (7) and confirmed by us during the course of these studies (26). The appearance of new peaks and the stable presence of other peaks from 7 to 13 d after clone 13 infection indicated that some T cells remained activated instead of undergoing clonal exhaustion during this period of time. However, the majority of these T cells eventually underwent clonal exhaustion long after the initial infection by continuous stimulation with excess viral antigens, as most spectratypes became like those of naive mice; only very weakly skewed spectratypes could occasionally be detected at 42 d after clone 13 infection (Fig. 7 *B*). Taken together, these results suggest that no further selection of LCMV-specific T cells occurs during the apoptosis phase in acute LCMV infection, although a continuous selection of LCMV-specific T cells does occur in the presence of excess viral antigens in LCMV clone 13 infection.

A previous, unresolved question was to what degree the specific immune response contracts after a systemic virus infection. Our spectratype data show that the LCMV infection substantially skews the host T cell repertoire in the memory state, as dominant peaks from the acute infection remain present. The immune spectratype 6–8 wk after infection is very different from that of naive mice, but resembles the combination of that of acutely infected and naive mice (Fig. 9 *A*). Thus, a host's T cell repertoire can be substantially altered by a virus infection, and remains skewed after the virus has been cleared. This molecular analysis is consistent with previous observations revealed by LDA and by quantification of transgenic T cells showing that LCMV infection leaves the host T cell repertoire with a very high frequency of LCMV-specific T cells (9, 12, 27), a claim also supported by a recent report on MHC-tetramer binding studies. However, here we have been able to show how a multiclonal T cell repertoire evolves from acute infection and is preserved in the memory state.

pCTL data have shown that the frequency of the LCMV-specific pCTL remains stable throughout the lifetime of the mouse (9, 12). In this study, we have examined the preservation of the LCMV-induced Vβ8.1 spectratype up to 7 mo after infection. We found that the relative intensity of a dominant peak within that specific spectrum was weaker at 4 mo than at 6–7 wk after LCMV infection (data not shown), but thereafter remained stable at least

through 7 mo of infection (Fig. 9 *B*). This may reflect the ability of RT-PCR to measure mRNA levels, which were probably reduced in the older memory cells, as incubation of the immune spleen cells or PB leukocytes with IL-2 rapidly revealed a spectratype similar to that of the acute infection (data not shown).

A broad spectrum of Vβ8.1$^+$ T cells was activated during acute LCMV infection (Fig. 3). A previous report examining specific T cell clones to Epstein-Barr virus suggested that an immunodominant epitope induced a broad T cell repertoire and that a subdominant epitope induced a more restricted T cell repertoire (28). The Vβ8$^+$ T cells recognize three LCMV immunodominant peptides (Table 1), so it is not surprising that a broad spectrum of T cells were activated during acute LCMV infection. Since dominant peaks in the acute infection are present in the immune state, it also appears that a broad repertoire of LCMV-specific T cells can be selected into memory. Some CTL clones isolated from LCMV-immune mice infected with serologically unrelated viruses, such as vaccinia virus or PV, cross-react between the two viruses (29). A broad spectrum of LCMV-specific memory T cells enhances the probability of having cross-reactive memory cell clones that can be stimulated and expanded quickly in the event of a second virus infection, thus providing protective immunity or influencing the pathogenesis of a second infection. Experiments have, in fact, demonstrated that a history of LCMV infection provides protective immunity against vaccinia virus, PV, and murine cytomegalovirus by controlling the viral replication early in infection (1). This examination of the Vβ8.1 TCR usage suggests that the majority of the dominant T cell clones detectable by spectratyping is not eliminated during the apoptosis phase and survive in the memory cell population.

The fact that the spectratypes of immune splenocytes and PB resemble a combination of the spectratypes found in these compartments of acutely infected and naive mice suggests that virus-specific memory cells become diluted with naive cells, a result consistent with our LDA analyses (9). However, the immune PEC have a spectratype virtually identical to that of the lymphoid compartments during the acute infection, which is consistent with the observation that immune PEC contained a very high frequency of LCMV-specific T cells (25). This result could be due to the fact that there is a lack of dilution of the memory cells with naive cells in the peritoneal cavity. Alternatively, the LCMV-specific memory T cells may be more likely to circulate back to the initial peritoneal cavity inoculation site. It is also possible that some viral antigens remain in the peritoneal cavity to provide continuous stimulation to the LCMV-specific T cells, such that they express a higher level of TCR RNA.

A recent study of the functional fine specificity of the LCMV-specific CTL response led Bachmann et al. (30) to propose that many T cells were deleted from the repertoire during the apoptosis phase of the primary LCMV infection. Previously published LDA data (9) as well as our data here showing that the spectratype and the examined TCR sequences remained stable during the apoptosis phase of the primary infection (Figs. 5 and 6) are inconsistent with that suggestion. However, they do not rule out the possibility that weak T cell responses insufficient to register in LDA or spectratype analyses were eliminated during this time period. Nevertheless, our data would indicate that changes in the T cell repertoire between the primary and secondary infections are not a consequence of the apoptotic phase of infection, but instead are due to the selective pressure of antigen during secondary infection.

An observation that we found of great interest is that even though genetically identical mice generate similar levels of CTL responses against the LCMV immunodominant peptides (9, 13), the TCR repertoire generating these responses differed from mouse to mouse (Fig. 3). Differences in spectratypes were even seen in LCMV-infected, α/β TCR-deficient mice reconstituted with a common pool of euthymic mouse splenocytes, supporting the argument that these differences were not caused by prior exposure to different antigens by the individual mice (data not shown). C57BL/6 mice infected with the same dose of LCMV had different spectratypes (Fig. 3). There was preferential Jβ usage and some homogeneity in the CDR3 length, but sequence analysis of the same sized discrete Vβ8.1-Jβ1.6 spectratype peaks revealed different DNA sequences. Although the DNA sequences were different, a conserved GXXN amino acid motif was detected in all the sequences analyzed, suggesting the importance of both the CDR3 length and this motif for the recognition of LCMV. Direct sequencing of dominant spectratype bands may be a useful technique to define conserved motifs associated with regions of the TCR involved in binding to the peptide–MHC complex. These observations are complementary to that of Maryanski et al. (31), who found that each of the mice immunized with the P815-CW3 cells displayed distinct but structurally similar CD8$^+$ TCR repertoires to the HLA-CW3 170-179 epitope, in that they had similar CDR3 length and displayed a conserved non-V, non-J–encoded glycine residue. A stochastic effect may play an important role in the differences of T cell responses to the same antigens. The fact that genetically identical hosts generate different T cell responses to the same antigens may help explain the variation of incidence in virus-induced autoimmune diseases in genetically identical hosts. For example, ~30% of the diabetes-resistant BB/Wor rats developed diabetes after Kilham's rat virus infection (32).

In summary, the data presented here indicate that genetically identical hosts generate remarkably different T cell responses to the same antigens and that studies on the evolution of the T cell repertoire require following the same individual hosts longitudinally during an antigenic challenge. Data from such a longitudinal study support the concepts that the virus-induced T cell repertoire remains stable both after clearance of the virus and during the apoptosis phase of the T cell response but evolves in the presence of the viral antigens, as shown in the clone 13 model and during secondary LCMV infection. A multiclonal T cell response induced during an infection is preserved into memory and continues to markedly skew the host T cell repertoire long after the virus has been cleared.

We would like to thank Drs. Liisa K. Selin and Eva Szomolanyi-Tsuda for valuable discussions, Jie Yin for excellent technical assistance, and Phyllis Spatrick and Barbara Eddy for DNA sequencing.

This work was supported by National Institutes of Health grants AI-17672 and AR-35506 to R.M. Welsh.

Address correspondence to Dr. Raymond Welsh, Department of Pathology, University of Massachusetts Medical School, 55 Lake Avenue North, Worcester, MA 01655. Phone: 508-856-5819; Fax: 508-856-5780; E-mail: RWelsh@bangate.ummed.edu

Received for publication 6 April 1998 and in revised form 18 August 1998.

References

1. Welsh, R.M., M.Y. Lin, B.L. Lohman, S.M. Varga, C.C. Zarozinski, and L.K. Selin. 1997. αβ and γδ T cell networks and their roles in natural resistance to viral infections. *Immunol. Rev.* 159:79–93.
2. Kalams, S.A., R.P. Johnson, M.J. Dynan, K.E. Hartman, T. Harrer, E. Harrer, A.K. Trocha, W.A. Blattner, S.P. Buchbinder, and B.D. Walker. 1996. T cell receptor usage and fine specificity of human immunodeficiency virus 1–specific cytotoxic T lymphocyte clones: analysis of quasispecies recognition reveals a dominant response directed against a minor in vivo variant. *J. Exp. Med.* 183:1669–1679.
3. Steven, N.M., A.M. Leese, N.E. Annels, S.P. Lee, and A.B. Rickinson. 1996. Epitope focusing in the primary cytotoxic T cell response to Epstein-Barr virus and its relationship to T cell memory. *J. Exp. Med.* 184:1801–1813.
4. Yanagi, Y., R. Maekawa, T. Cook, O. Kanagawa, and M.B.A. Oldstone. 1990. Restricted V-segment usage in T-cell receptors from cytotoxic T lymphocytes specific for a major epitope of lymphocytic choriomeningitis virus. *J. Virol.* 64:5919–5926.
5. Okamoto, Y., S.J. Gagnon, I. Kurane, A.M. Leporati, and F.A. Ennis. 1994. Preferential usage of T-cell receptor Vβ 17 by dengue virus–specific human T lymphocytes in a donor with immunity to dengue virus type 4. *J. Virol.* 68:7614–7619.
6. Ahmed, R., A. Salmi, L.D. Butler, J.M. Chiller, and M.B.A. Oldstone. 1984. Selection of genetic variants of lymphocytic choriomeningitis virus in spleens of persistently infected mice. *J. Exp. Med.* 160:521–540.
7. Moskophidis, D., F. Lechner, H. Pircher, and R.M. Zinkernagel. 1993. Virus persistence in acutely infected immunocompetent mice by exhaustion of antiviral cytotoxic effector T cells. *Nature.* 362:758–761.
8. Matloubian, M., S.R. Kolhekar, T. Somasundaram, and R. Ahmed. 1993. Molecular determinants of macrophage tropism and viral persistence: importance of single amino acid changes in the polymerase and glycoprotein of lymphocytic choriomeningitis virus. *J. Virol.* 67:7340–7349.
9. Selin, L.K., K. Vergilis, and R.M. Welsh. 1996. Reduction of otherwise remarkably stable virus-specific cytotoxic T lymphocyte memory by heterologous viral infections. *J. Exp. Med.* 183:2489–2499.
10. Razvi, E.S., and R.M. Welsh. 1993. Programmed cell death of T lymphocytes during acute viral infection: a mechanism for virus-induced immune deficiency. *J. Virol.* 67:5754–5765.
11. Razvi, E.S., Z. Jiang, B.A. Woda, and R.M. Welsh. 1995. Lymphocyte apoptosis during the silencing of the immune response to acute viral infections in normal, lpr, and Bcl-2-transgenic mice. *Am. J. Pathol.* 147:79–91.
12. Lau, L.L., B.D. Jamieson, T. Somasundaram, and R. Ahmed. 1994. Cytotoxic T-cell memory without antigen. *Nature.* 369:648–652.
13. Murali-Krishna, K., J.D. Altman, M. Suresh, D.J.D. Sourdive, A.J. Zajac, J.D. Miller, J. Slansky, and R. Ahmed. 1998. Counting antigen-specific CD8 T cells: a reevaluation of bystander activation during viral infection. *Immunity.* 8:177–187.
14. Zarozinski, C.C., and R.M. Welsh. 1997. Minimal bystander activation of CD8 T cells during the virus-induced polyclonal T cell response. *J. Exp. Med.* 185:1629–1639.
15. Pannetier, C., J. Evan, and P. Kourilsky. 1995. T-cell repertoire diversity and clonal expansions in normal and clinical samples. *Immunol. Today.* 16:176–181.
16. Bjorkman, P.J. 1997. MHC restriction in three dimensions: a view of T cell receptor/ligand interaction. *Cell.* 89:167–170.
17. Welsh, R.M., P.W. Lampert, P.A. Burner, and M.B.A. Oldstone. 1976. Antibody-complement interactions with purified lymphocytic choriomeningitis virus. *Virology.* 73:59–71.
18. Planz, O., P. Seiler, H. Hengartner, and R.M. Zinkernagel. 1996. Specific cytotoxic T cells eliminate cells producing neutralizing antibodies. *Nature.* 382:726–729.
19. Nahill, S.R., and R.M. Welsh. 1993. High frequency of cross-reactive cytotoxic T lymphocytes elicited during the virus-induced polyclonal cytotoxic T lymphocyte response. *J. Exp. Med.* 177:317–327.
20. Selin, L.K., and R.M. Welsh. 1997. Cytolytically active memory CTL present in lymphocytic choriomeningitis virus–immune mice after clearance of virus infection. *J. Immunol.* 158:5366–5373.
21. Welsh, R.M. 1978. Cytotoxic cells induced during lymphocytic choriomeningitis virus infection of mice. I. Characterization of natural killer cell induction. *J. Exp. Med.* 148:163–181.
22. Pannetier, C., M. Cochet, S. Darche, A. Casrouge, M. Zöller, and P. Kourilsky. 1993. The sizes of the CDR3 hypervariable regions of the murine T-cell receptor β chains vary as a function of the recombined germ-line segments. *Proc. Natl. Acad. Sci. USA.* 90:4319–4323.
23. Chomczynski, P., and N. Sacchi. 1987. Single-step method of RNA isolation by acid guanidinium thiocyanate-phenol-chloroform extraction. *Anal. Biochem.* 162:156–159.
24. Blüthmann, H., P. Kisielow, Y. Uematsu, M. Malissen, P. Krimpenfort, A. Berns, H. von Boehmer, and M. Steinmetz. 1988. T-cell–specific deletion of T-cell receptor transgenes allows functional rearrangement of endogenous α- and β-genes. *Nature.* 334:156–159.
25. McFarland, H.I., S.R. Nahill, J.W. Maciaszek, and R.M.

Welsh. 1992. CD11b (Mac-1): a marker for $CD8^+$ cytotoxic T cell activation and memory in virus infection. *J. Immunol.* 149:1326–1333.
26. Lohman, B.L., and R.M. Welsh. 1998. Apoptotic regulation of T cells and absence of immune deficiency in virus-infected IFN-γ receptor knock-out mice. *J. Virol.* 72:7815–7821.
27. Zimmermann, C., K. Brduscha-Riem, C. Blaser, R.M. Zinkernagel, and H. Pircher. 1996. Visualization, characterization, and turnover of $CD8^+$ memory T cells in virus-infected hosts. *J. Exp. Med.* 183:1367–1375.
28. de Campos-Lima, P.O., V. Levitsky, M.P. Imreh, R. Gavioli, and M.G. Masucci. 1997. Epitope-dependent selection of highly restricted or diverse T cell receptor repertoires in response to persistent infection by Epstein-Barr virus. *J. Exp. Med.* 186:83–89.
29. Selin, L.K., S.R. Nahill, and R.M. Welsh. 1994. Cross-reactivities in memory cytotoxic T lymphocyte recognition of heterologous viruses. *J. Exp. Med.* 179:1933–1943.
30. Bachmann, M.F., D.E. Speiser, and P.S. Ohashi. 1997. Functional maturation of an antiviral cytotoxic T-cell response. *J. Virol.* 71:5764–5768.
31. Maryanski, J.L., C.V. Jongeneel, P. Bucher, J.L. Casanova, and P.R. Walker. 1996. Single-cell PCR analysis of TCR repertoires selected by antigen in vivo: a high magnitude CD8 response is comprised of very few clones. *Immunity.* 4:47–55.
32. Guberski, D.L., V.A. Thomas, W.R. Shek, A.A. Like, E.S. Handler, A.A. Rossini, J.E. Wallace, and R.M. Welsh. 1991. Induction of type I diabetes by Kilham's rat virus in diabetes-resistant BB/Wor rats. *Science.* 254:1010–1013.
33. Chou, H.S., S.J. Anderson, M.C. Louie, S.A. Godambe, M.R. Pozzi, M.A. Behlke, K. Huppi, and D.Y. Loh. 1987. Tandem linkage and unusual RNA splicing of the T-cell receptor β-chain variable-region genes. *Proc. Natl. Acad. Sci. USA.* 84:1992–1996.